JACS
JOURNAL OF THE AMERICAN CHEMICAL SOCIETY

Article

pubs.acs.org/JACS

Insights into the Mechanism by Which Interferon-γ Basic Amino Acid Clusters Mediate Protein Binding to Heparan Sulfate

Els Saesen,[†] Stéphane Sarrazin,[†,§] Cédric Laguri,[†] Rabia Sadir,[†] Damien Maurin,[†] Aline Thomas,[‡] Anne Imberty,[‡] and Hugues Lortat-Jacob*[,†]

[†]Institut de Biologie Structurale, CNRS, CEA, University Grenoble Alpes, UMR 5075, 41 rue Horowitz, 38027, Grenoble cedex 01, France

[‡]Centre de Recherches sur les Macromolécules Végétales, CNRS UPR 5301 (affiliated with Université Joseph Fourier), 38041, Grenoble cedex 09, France

Supporting Information

ABSTRACT: The extensive functional repertoire of heparin and heparan sulfate, which relies on their ability to interact with a large number of proteins, has recently emerged. To understand the forces that drive such interactions the binding of heparin to interferon-γ (IFNγ), used as a model system, was investigated. NMR-based titration experiments demonstrated the involvement of two adjacent cationic domains (D1: KTGKRKR and D2: RGRR), both of which are present within the carboxy-terminal sequence of the cytokine. Kinetic analysis showed that these two domains contribute differently to the interaction: D1 is required to form a complex and constitutes the actual binding site, whereas D2, although unable to associate with heparin by itself, increased the association rate of the binding. These data are consistent with the view that D2, through nonspecific electrostatic forces, places the two molecules in favorable orientations for productive binding within the encounter complex. This mechanism was supported by electrostatic potential analysis and thermodynamic investigations. They showed that D1 association to heparin is driven by both favorable enthalpic and entropic contributions, as expected for a binding sequence, but that D2 gives rise to entropic penalty, which opposes binding in a thermodynamic sense. The binding mechanism described herein, by which the D2 domain kinetically drives the interaction, has important functional consequences and gives a structural framework to better understand how specific are the interactions between proteins and heparin.

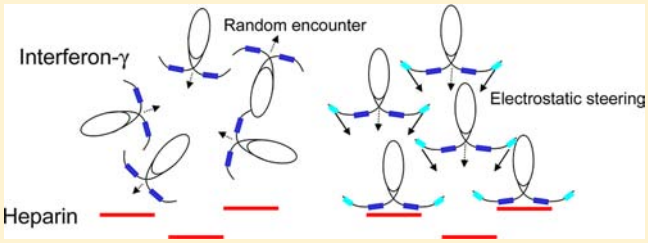

INTRODUCTION

Heparan sulfate (HS) is a large anionic polysaccharide that is widely present in the pericellular zone, where it is attached to cell surface or extracellular matrix-associated proteins. Over the past two decades, this glycosaminoglycan (GAG) has emerged as a key regulator of most biological processes, including cell proliferation and development, chemoattraction, inflammation and immune response, lipid metabolism, angiogenesis, matrix assembly, or viral attachment.[1] HS does so by interacting with a vast array of proteins, thereby modulating their conformation, stability, local concentration, and bioactivity or acting as a template for the assembly of active supramolecular complexes.[2] Such interactions play critical roles, for example, in assembling growth factor−receptor complexes involved in cell signaling,[3] mediating the formation of chemotactic gradients (thus enabling the oriented migration of cells) or protecting cytokines against proteolysis.[4−7]

These multiple binding activities are closely related to the structural features of HS. It consists of repeating units of hexuronic acid (D-glucuronic or L-iduronic acid) and D-glucosamine, in which biosynthetically imprinted, highly *O*- and *N*-sulfated domains provide distinct docking sites for proteins.[2] Given the high content of charged groups in these domains, which have the highest negative charge density of any known biological macromolecules, it is not surprising that protein binding is generally (but not exclusively) driven by electrostatic interactions. Electrostatics play an important part in molecular recognition because of their long-range nature and their ability to form favorable charge−charge interactions between the substrate and the ligand.[8] Early studies based on HS binding-protein sequence comparisons[9] led to the proposal of a number of HS binding consensus motifs, such as BBXB or BBBXXB, where B stands for a basic and X for a neutral/hydrophobic amino acid. This does not exclude HS binding epitopes that comprise distant amino acids organized in a precise orientation through the folding of the protein[10,11] or the contribution of other more directional and short-range forces such as van der Waals interactions and hydrogen bonds. However, beyond forming small clusters of Lys and Arg residues that can establish salt bridges with spatially defined negative charges on HS chains, only limited information is available on the mechanism through which amino acid sequences determine interaction with HS.

Received: January 10, 2013
Published: June 4, 2013

   dx.doi.org/10.1021/ja4000867 | J. Am. Chem. Soc. 2013, 135, 9384−9390

Here, to better understand how basic amino acid clusters contribute to protein−HS binding and the forces that drive such interactions, we focused our attention on interferon-γ (IFNγ). This homodimeric cytokine, predominantly produced by natural killer cells and some T-lymphocytes, is a known GAG binding protein,[12−14] which coordinates a remarkably large array of cellular functions.[15] In particular, IFNγ plays a central role in both innate and adaptive immune responses, and it is important in early host defense against pathogens.[16] IFNγ binding to HS determines its local concentration within tissues[17] and controls its biological activity.[18−20] The HS binding site of this cytokine, located within the carboxy-terminal domain of the protein, comprises two adjacent clusters of basic residues, D1 (KTGKRKR) and D2 (RGRR)[21] of which the individual contributions remain unknown.

We thus engineered a number of IFNγ carboxy terminal mutants and examined, using electrostatic potential calculation, NMR, surface Plasmon resonance (SPR,) and isothermal titration calorimetry (ITC)-based methods, their interaction with HS. We report that both clusters are critically involved in HS binding, but while D1 constitutes the actual HS binding domain, D2 mostly functions by enhancing the association rate of the complex. This mechanism has important functional consequences, and combined with data showing that D1 but not D2 is also involved in the binding to IFNγR (the cell surface signaling receptor), it provides a model by which HS controls the cytokine activity.

EXPERIMENTAL SECTION

IFNγ Mutagenesis, Expression, and Purification. Human IFNγ cDNA was cloned into a pET11a expression vector and used as a template for mutagenesis. This was performed with the quick change II Site-Directed Mutagenesis Kit, as described in the manufacturer's instructions. Wild-type and mutant vectors were characterized by DNA sequencing and used to transform *E. coli* strain BL21 Star DE3. Cells were grown at 37 °C in Luria broth medium containing 100 μg/mL ampicillin and induced with 0.5 mM isopropyl 1-thio-β-D-galactopyranoside for 5 h. For isotopic enrichment, cells were grown in M9 minimal medium supplemented with $^{15}NH_4Cl$ and ^{13}C-glucose. Purification from inclusion bodies was performed as described in the Supporting Information (SI).

Preparation and Characterization of Heparin-Derived Oligosaccharides. Heparin-derived di (dp2)-, tetra (dp4)-, and octa (dp8)-saccharides were prepared from heparinase I digested porcine mucosal heparin as described in the SI. NMR analysis of these materials indicated the following structure: ΔHexA2S-[GlcNS6S-IdoA2S]$_n$-GlcNS6S, with n = 0, 1, or 3 for dp2, dp4, or dp8, respectively.

NMR Experiments. NMR experiments were recorded at 27 °C in NaH_2PO_4 (20 mM) pH 6.0, 10% D_2O buffer on cryoprobe-equipped 600 and 800 MHz Varian spectrometers. Backbone assignment of the IFNγ carboxy terminus was performed on a $^{15}N^{13}C$-labeled sample (1.2 mM) using the ASCOM approach[22] to record highly folded 4D HNCOCACB and CBCACONH. Assignment of the IFNγ first 125 residues was transferred from the NMR study of Grzesiek et al.[23] In titration experiments heparin-derived oligosaccharides (9 mM) were progressively added to an IFNγ sample (54 μM for dp4 and dp8 titrations and 72 μM for dp2 titration) in the above-mentioned buffer, and ^{15}N-HSQCs experiments were recorded. The resulting data were processed with NMRpipe and analyzed with NMRview and ccpnmr. Nonlinear curve fitting of chemical shift variations upon oligosaccharide interaction was performed with xmgrace using the equation:

$$\mathrm{dHN} = \mathrm{dHN}_{max} * ((L + P + K_{dapp}) - \sqrt{((L + P + K_{dapp})^2 - (4 * P * L))})/p * 2$$

where dHN is the chemical shift variation and P and L are the protein and ligand concentration, respectively.

Biotinylation Procedures and Surface Plasmon Resonance Based-Binding Assays. Heparin (9 kDa), HS (12 kDa), and the soluble IFNγR were biotinilated as detailed in the SI and capture to a level of 40, 50, and 800 RU, respectively, on a streptavidin surface prepared as previously described.[24] For binding assays, IFNγ in HBS-EP buffer was injected at 60 μL/min over both a negative control and heparin, HS, or IFNγR surfaces for 4 min at 25 °C. The binding curves were evaluated with the Biaevaluation 3.1 software, and for the IFNγ-IFNγR interaction the data were analyzed by fitting both association and dissociation phases for several IFNγ concentrations. The affinities (dissociation equilibrium constants: K_D) were calculated from the ratio of dissociation and association rate constants ($K_D = k_{off}/k_{on}$). In some cases (IFNγ − heparin interaction, where global fitting was not possible − see below), k_{off} and k_{on} were determined independently. In those cases, K_D were also estimated both by fitting the steady state values at equilibrium (R_{eq}) assuming one binding site with $R_{eq} = R_{max_{eq}}/(K_D + c)$, and by plotting Req/$c$ against Req for different IFNγ concentrations (c).

Electrostatic Potential of IFNγ. Electrostatic potential of IFNγ, IFNγ$_{Δ136}$, and IFNγ$_{Δ124}$ were calculated using the Adaptive Poisson−Boltzmann Solver (APBS) tools as implemented in the Pymol software (www.pymol.org). Hydrogen atoms and partial charges at pH 7 were computed in APBS plugin with PDB2PQR software approach.[25] Electrostatic potential was calculated using APBS[26] for 150 mM ionic strength with a protein dielectric of 2 and a solvent dielectric of 78.5 by using the same grid of 300 Å × 300 Å × 150 Å for the three proteins. Dipole moments were calculated at the Protein Dipole Moments Server (http://bioinfo.weizmann.ac.il/dipol/).[27]

Titration Microcalorimetry Measurements. ITC experiments were performed at 25 °C with a VP-ITC isothermal titration calorimeter (Microcal). IFNγ and heparin-derived octasaccharide (dp8) were prepared in PBS (pH 7.2). IFNγ concentrations in the microcalorimeter cell (1.4478 mL) were 20 μM for the wt and 100 μM for IFNγ$_{Δ136}$, in order to give c values of 20 and 10, respectively. Aliquots of 10 μL dp8 solution (112.5 μM and 1 mM for IFNγ and IFNγ$_{Δ136}$ titration, respectively) were added at intervals of 5 min while stirring at 310 rpm. The experimental data were integrated and fitted to a theoretical single-binding site titration curve using MicroCal Origin 7 software to determine changes in enthalpy ($ΔH$), entropy ($ΔS$), and free energy ($ΔG$). The association constant (K_A) was calculated from the equation $ΔG = ΔH − TΔS = −RT \ln K_A$ (with T the absolute temperature and R = 8.314 J mol^{-1} K^{-1}).

IFNγ Bioassay. Antiviral activity was determined in triplicate with a standard microtiter inhibition-of-cytopathic-effect assay against the vesicular stomatitis virus (VSV) on monolayers of WISH cells as detailed in the Supporting Information.

RESULTS AND DISCUSSION

Both D1 and D2 Domains of the IFNγ Carboxy Terminus Are Targeted by Heparin-Derived Oligosaccharides. The carboxy-terminal domain of IFNγ comprises two clusters of basic amino acids (referred to as D1: KTGKRKR, residues 125−131 and D2: RGRR, residues 137−140), for which the respective importance for HS binding has not been determined. The involvement of these two clusters in HS binding was first evaluated by NMR spectroscopy. For that purpose, IFNγ was purified from bacteria grown in $^{15}NH_4Cl$ and ^{13}C-glucose supplemented medium, and the backbone resonances were assigned (Figure S1 in SI). The $^{15}N-^{1}H$ correlation spectra of the IFNγ were then recorded upon titration experiments with heparin-derived di (dp2)-, tetra (dp4)-, and octa (dp8)-saccharides. Significant changes in the chemical shift of IFNγ amide groups were observed upon binding in both the $K^{128}-R^{137}$ and $R^{140}-A^{141}$ regions of the carboxy-terminal domain (Figure 1).

dx.doi.org/10.1021/ja4000867 | J. Am. Chem. Soc. 2013, 135, 9384−9390

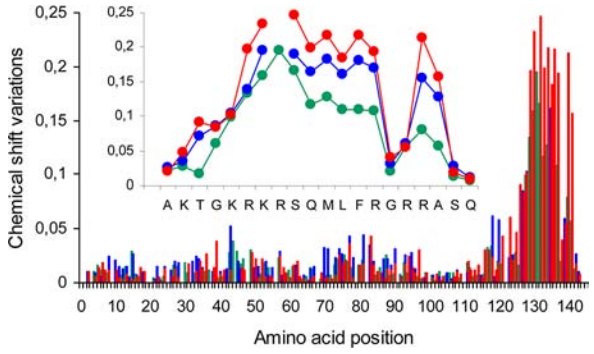

Figure 1. Chemical shift variation of IFNγ upon binding HP-derived oligosaccharides. Weighted chemical shift differences ($\sqrt{((\Delta\delta H)^2 + (\Delta\delta N/10)^2)}$) of IFNγ amide protons upon addition of dp2 (green), dp4 (blue), or dp8 (red) at oligosaccharide/IFNγ molar ratios of 8.2, 3.7, and 1.1, respectively. (Inset) Chemical shift variations of the IFNγ C-terminal sequence.

To determine the apparent affinity (K_{Dapp}) at the residue level, the evolution of the $^{15}N-^{1}H$ chemical shifts with the protein/oligosaccharide molar ratio was followed (Figure S1 in SI) and fitted to a standard binding equation (see Experimental Section). On average, the dp2 featured an affinity in the range of ~100 μM (data not shown), whereas that of the dp4 was 30 μM for K^{128}, 53 μM for K^{130}, and 140 μM for R^{137}. The binding of dp8 to IFNγ showed a linear evolution during complex formation with a saturating binding curve at approximately 1:1 protein/oligosaccharide ratio (data not shown). This suggested that the affinity was much lower than the protein concentration (50 μM) and thus could not be measured in the conditions required by this experiment. These data suggest that the K^{128}–K^{130} (D1) is the most favorable area for interaction with the oligosaccharides, whereas the residues of the D2 domain (R^{137}) are less active. The chemical shift perturbations of residue A^{141}, which displayed a sigmoid curve during the titration (Figure S1 in SI), also suggested that residues of the D2 domain required higher oligosaccharide concentrations than the D1 domain to be targeted. Taken together, these data indicate that both the D1 and D2 domains of the IFNγ C-terminus are perturbed by heparin-derived oligosaccharides and suggest that D1 is the predominant binding site.

Basic Amino Acids within D1 and D2 Domains Contribute Differently to Heparin Binding. To confirm the involvement of residues from both the IFNγ D1 and D2 domains in heparin recognition, different types of IFNγ mutants were engineered (Table 1). $IFN\gamma_{\Delta136}$ and $IFN\gamma_{\Delta124}$ are deletion mutants lacking the 137–143 and 125–143 C-terminal sequences, respectively. $IFN\gamma_{SD1}$ and $IFN\gamma_{SD2}$ are mutants in which all the basic amino acid residues of D1 and D2 clusters respectively were substituted by a serine. Finally, $IFN\gamma^{K125S}$, $IFN\gamma^{K128S}$, $IFN\gamma^{R129S}$, $IFN\gamma^{K130S}$, $IFN\gamma^{K131S}$, $IFN\gamma^{R137S}$, $IFN\gamma^{R139S}$, and $IFN\gamma^{R140S}$ are single amino acid mutants. These samples were all obtained with a very good degree of purity (>95%; data not shown), characterized by mass spectrometry (Table 1) and quantified by amino acid analysis.

Affinity for heparin was determined using a solid-phase assay that mimics, to some extent, the cell membrane-anchored HS. For that purpose, reducing end biotinylated heparin was immobilized on top of a streptavidin-coated sensorchip, and surface plasmon resonance (SPR) monitoring was used to measure changes in refractive index caused by the interaction,

Table 1. Wild-Type- and Mutant-IFNγ Carboxy-Terminal Sequences[a]

Name	IFNγ Carboxy-terminal sequence (D1 / D2)	MM^{exp}	MM^{mea}
$IFN\gamma_{wt}$	AKTG**KRKR**SQMLF**RGRR**ASQ	16907.3	16907.7
$IFN\gamma_{\Delta124}$	A	14633.6	14634.2
$IFN\gamma_{\Delta136}$	AKTG**KRKR**SQMLF	16095.4	16096.1
$IFN\gamma_{SD1}$	ASTGSSSSSQMLF**RGRR**ASQ	16645.8	16645.4
$IFN\gamma_{SD2}$	AKTG**KRKR**SQMLFSGSSASQ	16700.0	16700.8
$IFN\gamma^{K125S}$	ASTG**KRKR**SQMLF**RGRR**ASQ	16866.2	16866.7
$IFN\gamma^{K128S}$	AKTGS**RKR**SQMLF**RGRR**ASQ	16866.2	16866.6
$IFN\gamma^{R129S}$	AKTGKS**KR**SQMLF**RGRR**ASQ	16838.2	16838.7
$IFN\gamma^{K130S}$	AKTG**KR**SRSQMLF**RGRR**ASQ	16866.2	16866.6
$IFN\gamma^{R131S}$	AKTG**KRK**SSQMLF**RGRR**ASQ	16838.2	16838.4
$IFN\gamma^{R137S}$	AKTG**KRKR**SQMLFSGRRASQ	16838.2	16838.6
$IFN\gamma^{R138S}$	AKTG**KRKR**SQMLF**RG**SRASQ	16838.2	16838.7
$IFN\gamma^{R140S}$	AKTG**KRKR**SQMLF**RGR**SASQ	16838.2	16838.6

[a]The carboxy-terminal sequence of human IFNγ (amino acids 124–143) is enriched in basic residues (bolded) clustered in two domains (referred here as D1 and D2). The sequence of the different mutants used (mutated residues are indicated in red) are shown as their expected (MM^{exp}) and measured (MM^{mea}) molecular masses.

when the cytokine samples were flowed across the immobilized heparin surface (Figure 2).

Preliminary analysis of the resulting sensorgrams indicated that the interactions proceeded at high binding rates and were strongly dominated by mass transfer. Global fitting of the association and dissociation phases, therefore, did not permit an accurate simultaneous determination of the rate constants (see below). As the association phases were allowed to proceed to equilibrium, steady-state data were used in a first approach to determine affinity independently of the kinetic aspect of the binding (Figure S2 in SI). IFNγ had a high affinity for both heparin (K_D = 1.4 ± 0.2 nM) and HS (K_D = 2.4 ± 0.24 nM). These values are almost identical to that of ^{125}I-IFNγ for authentic basement membrane HS (1.5 nM).[14] Single-point mutations revealed that of the five basic residues within D1, K^{128}, R^{129}, K^{130}, and R^{131} more importantly contribute to the interaction (with K_D reduced to 9.9, 9.4, 7.9, and 9.4 nM, respectively) than K^{125} (K_D = 5.1 nM). Mutations of R^{137}, R^{139}, and R^{140} within D2 also reduced the affinity, with K_D of 4.3, 4.3, and 3.8 nM, respectively (Figure 3). Together, these results are consistent with the NMR titration experiments and further support that, of the two domains, D1 was the most important.

To better establish this point, $IFN\gamma_{\Delta136}$ (which lacks D2) and $IFN\gamma_{SD2}$ (in which the basic residues of D2 were mutated) were investigated. Injection of these two mutants using the same experimental conditions (0–15 nM) returned only weak binding. When injected at higher concentrations (0–150 nM), binding activity was observed (Figure 2E,F); however, equilibrium was reached after only 20 min (data not shown), suggesting a much lower association rate constant than that of the wt-cytokine (see below). For $IFN\gamma_{\Delta136}$, these data (Figure S2 in SI) provided an affinity value of 89 ± 8.1 nM (Figure 3). In contrast, $IFN\gamma_{SD1}$ (in which the basic residues of D1 were mutated) did not show any binding when injected in the 0–150 nM range (Figure 2L), nor did increasing its concentration to 1.5 μM. These results demonstrate that, collectively, the basic residues within D1 were essential to the interaction, as $IFN\gamma_{SD1}$

dx.doi.org/10.1021/ja4000867 | J. Am. Chem. Soc. 2013, 135, 9384–9390

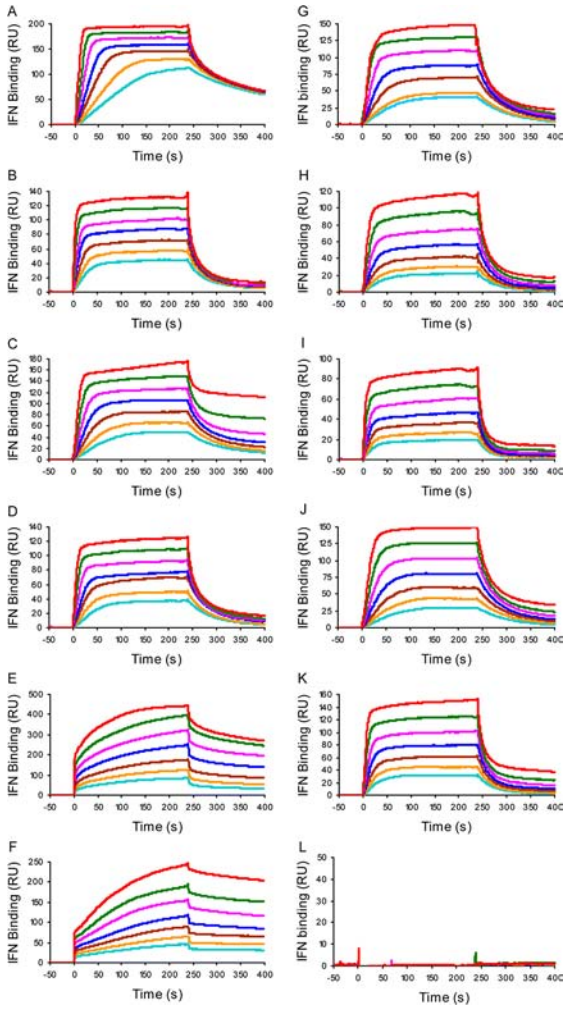

Figure 2. IFNγ binding to immobilized heparin. (A) wt-IFNγ, (B) IFNγ^{R137S}, (C) IFNγ^{R139S}, (D) IFNγ^{R140S}, (E) IFN$\gamma_{\Delta136}$, (F) IFNγ_{SD2}, (G) IFNγ^{K125S}, (H) IFNγ^{K128S}, (I) IFNγ^{R129S}, (J) IFNγ^{K130S}, (K) IFNγ^{R131S}, and (L) IFNγ_{SD1} were injected over a heparin-activated surface at a flow rate of 60 μL/ml, during 4 min, and the binding response in resonance units (RU) was recorded as a function of time. Each set of sensorgrams was obtained with wt- and a single-point mutant-IFNγ at (from top to bottom) 15, 10, 6.66, 4.44, 2.96, 1.98, and 1.32 nM (for A–D and G–K, respectively) and 150, 100, 66.6, 44.4, 29.6, 19.8, and 13.2 nM (for E, F, and L, respectively).

did not bind to heparin. This also reveals that D2, by itself, did not mediate specific binding of the cytokine, even at very high concentrations (1.5 μM). Nevertheless, in the presence of D1, D2 played a crucial role, as its removal (IFNγ_{136}) led to a 60-fold reduction in affinity.

The D2 Domain Enhanced the Association Rate of the IFNγ–heparin Interaction. To further assess the differences that characterize IFNγ and IFN$\gamma_{\Delta136}$ and thus the role of D2, the dissociation and association rate constants (k_{off} and k_{on}) of these two samples were measured. Our data, however, did not follow the expected ideal binding progress curve for a pseudo-first-order reaction, presumably because of important mass transport limitation and rebinding effect (see Figure S3 in SI). Global fitting of the association and dissociation phases, therefore, did not permit an accurate determination of the rate constants. To estimate nevertheless the kinetic parameters, the off-rates were first taken from the initial part of the dissociation phases (first 30 s where rebinding is limited

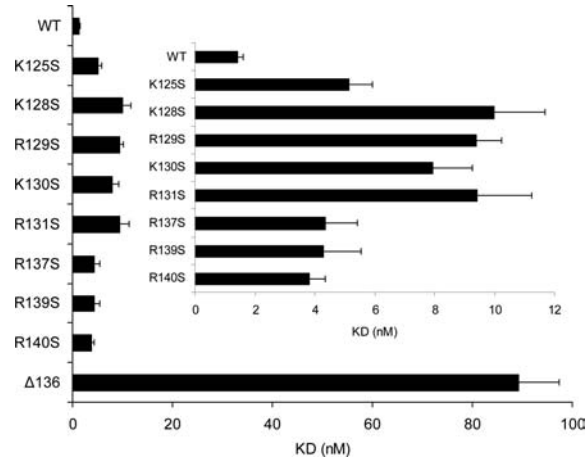

Figure 3. Equilibrium dissociation constant of wt- and mutant-IFNγ for heparin. Steady-state levels of bound IFNγ were extracted from the sensorgrams of Figure 2 at the end of the association phases (apart from the IFNγ_{SD2} and IFNγ_{SD1} which did not reach equilibrium), and the dissociation constants (K_D) were calculated by fitting the data to $R_{eq} = R_{max_{eq}}/(K_D + c)$. R_{eq} values are the steady-state values, and c is the concentration of injected proteins. Data were also analyzed using the Scatchard representation (see Figure S2 in SI). The histogram shows the K_D (in nM) as the means ± SEM of 3–4 experiments. (Inset) K_D for wt- and single-point mutant-IFNγ.

because the number of free immobilized heparin remains low). This returned k_{off} of 1.24 ± 0.07 × 10^{-2} S^{1-} and 4.84 ± 0.18 × 10^{-3} S^{1-} for IFNγ and IFN$\gamma_{\Delta136}$, respectively. These values were then used to fit part of the association phase that was not mass transport limited (Figure S3 in SI). This returned k_{on} of 7.83 ± 0.5 × 10^6 and 8.39 ± 0.9 × 10^4 M^{-1} S^{1-}, thus indicating that the presence of D2 increased the association rate constant by 2 orders of magnitude (Figure 4). Because they were not

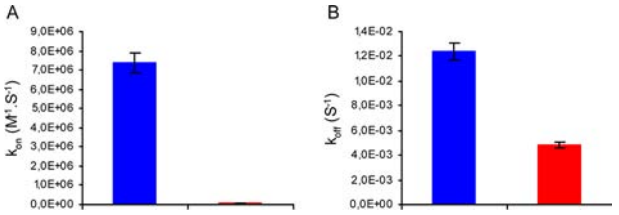

Figure 4. Association (A) and dissociation (B) rate constants of IFNγ and IFN$\gamma_{\Delta136}$ for heparin. Association (k_{on}) and dissociation (k_{off}) rate constants (the mean of two independent analyses) of IFNγ (blue) and IFN$_{\gamma\Delta136}$ (red) for heparin were determined by fitting the primary data of Figure 2 using Biaeval 3.1.

determined by global fitting (which provides a more stringent test of the assumed model and returns better parameter estimates than fitting only a portion of the binding data), these kinetic values should be considered as estimates only. It is worth noting, however, that they returned k_{off}/k_{on} ratio = K_D of 1.63 ± 0.16 and 75.8 ± 10.6 nM for IFNγ and IFN$\gamma_{\Delta136}$, respectively, which are very close to the steady-state data and validate to some extent the kinetic determination. Therefore, the D2 domain provides the cytokine with an enhanced and very high association rate constant but does not appear to be involved in the formed complex.

From a kinetic perspective, a binding process can be viewed as a two-step mechanism: diffusional association in which molecular encounters occur in orientations where the

dx.doi.org/10.1021/ja4000867 | J. Am. Chem. Soc. 2013, 135, 9384–9390

interacting domains of the partners are not necessarily into appropriate positions, followed by a series of translational or rotational motions within the so-called encounter complex, until a mutually reactive configuration is found, leading to specific association. In that context, it can be hypothesized that the D2 domain, through nonspecific electrostatic forces during the early stages of the binding reaction, contributes to increase the probability of productive encounters between IFNγ and heparin and thus achieve a higher interaction affinity.

Computational and experimental studies have shown already that clusters of basic residues enhance binding in protein−DNA[28,29] or protein−protein[30,31] interactions, by inducing precollision orientational effects that place the two molecules in a suitable configuration within the encounter complex. Implicit in the realization of such a mechanism is the existence of a significant imbalance in the spatial distribution of the charges on the protein, forming a large electrostatic dipole moment.

Electrostatic Potential of IFNγ. Models of full-length IFNγ and IFNγΔ_{136} were obtained from 2 ns simulations in explicit water (see SI), starting from the IFNγ (1−119) structure with the C-terminal sequence (residues 120−143 or 120−136) built as extended β-strands.[32] For both models, the C-terminal peptides relaxed from fully extended shape and stabililized in reasonable conformations (see Figure S4 in SI). These C-terminal models do not aim at representing the conformational space that could be covered by such flexible C-terminal peptides but are compatible with biophysical data previously obtained for IFNγ interacting with anionic polysaccharide.[32]

Electrostatic properties of these two models, and that of IFNγΔ_{124}, were calculated using APBS.[26] Although IFNγ features two others basic clusters (KLFKNFK and KKKR, residues 55−61 and 86−89, respectively), this analysis indicated that D1 and D2 induce a strong asymmetry in charge distribution, characterized by a very large positive electrostatic potential in the carboxy-terminal domain (Figure 5).

Calculations of protein dipole also illustrated the influence of D1 and D2. The IFNγ$_{\Delta124}$ mutant had a very small dipole moment (29 D), while that of IFNγ$_{\Delta136}$ was 823 D. This can be compared to the mean value of 639 D (median 452 D) calculated on approximately 12000 protein structures,[27] that is further enhanced to 983 D on wt-IFNγ. In IFNγ the orientation of the dipole moment is parallel to the 2-fold axis and perpendicular to the extended carboxy-terminal regions, such that it can attract negatively charged species toward the correct binding site (Figure S5 in SI).

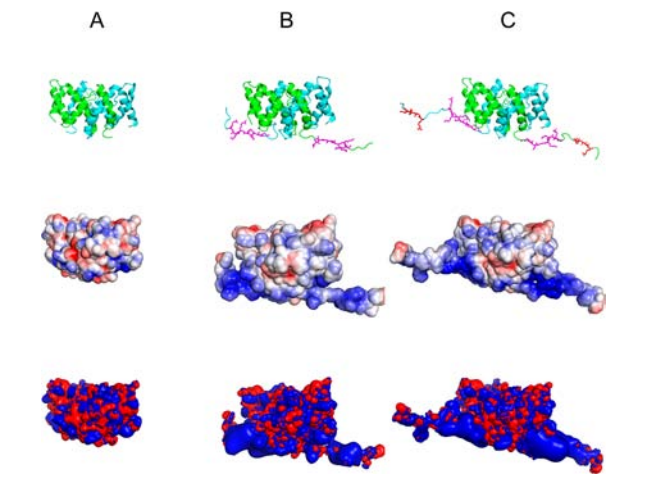

Figure 5. Structural model and electrostatic potential of IFNγ. (Top) ribbon representation of (A) IFNγ$_{\Delta124}$ (PDB entry 1HIG), (B) IFNγ$_{\Delta136}$ and (C) wt-IFNγ protein. (Middle) Electrostatic potential mapped on the solvent accessible surface. Values are expressed as a color spectrum ranging from +3 kT/e (blue) to −3 kT/e (red). (Bottom) Potential isocontours shown at +2 kTye (blue) and −2 kTye (red).

A number of observations support this view. First, removal of the D2 domain has a major effect on the association phase of the reaction, demonstrating that D2 is indeed more active during the complex formation (diffusional association through long-range nonspecific interactions) than within the formed complex. Next, early work showed that a synthetic peptide corresponding to D1 competes with IFNγ to bind HS but that a D2 peptide was ineffective.[21] Finally, once bound to heparin, the IFNγ D1- but not D2-domain is protected from protease-mediated cleavage, indicating that within the complex, D1 is tightly bound to heparin (presumably through pairwise short-range interactions), while D2 remains accessible.[20]

Thermodynamics of Heparin Binding to IFNγ. To further investigate the mechanism by which the IFNγ D1 and D2 clusters each contribute to heparin binding, the thermodynamic parameters characterizing the interactions for a sample comprising both domains (IFNγ) and a sample with only the D1 domain (IFNγ$_{\Delta136}$) were determined by ITC. A heparin derived-octasaccharide (dp8) was used for that purpose, because full-length heparin induced IFNγ precipitation at the concentration required for ITC measurements (data not shown).

The ITC profiles showed that the binding of the heparin dp8 to both IFNγ$_{\Delta136}$ and IFNγ was exothermic, resulting in negative peaks in the plots of power versus time (Figure 6). The signals were fitted to a single-site binding model to determine the K_D, enthalpy (ΔH), entropy (ΔS), and free energy (ΔG) changes of the binding reaction. Affinities of IFNγ$_{\Delta136}$ and IFNγ for heparin dp8 were 10.4 ± 0.51 μM and 0.41 ± 0.001 μM respectively, confirming the affinity enhancement provided by the D2 domain (with a $\Delta\Delta G$ of 8 kJ/mol).

Binding of IFNγ$_{\Delta136}$ to dp8 was contributed by both favorable entropy and enthalpy terms. This suggested that the D1 domain association to dp8 was not only driven by a large entropy gain ($T\Delta S$ = 10.4 ± 1.5 kJ/mol) presumably due to the release of adsorbed counterions during complexation which typically occurs in binding to polyelectrolytes[33] but also by hydrogen bonding and/or van der Waals and Coulombic interactions (ΔH = −18.0 ± 1.4 kJ/mol). Examination of the thermodynamic contribution of the wt-IFNγ binding indicated that the additional presence of the D2 domain generated, in contrast to D1, an unfavorable entropy term ($T\Delta S$ = −6.9 ± 1.8 kJ/mol) that was counterbalanced by a higher enthalpy change (ΔH = −43.4 ± 1.8 kJ/mol).

The D2 domain thus produced drastic changes in the thermodynamic parameters of the interaction, with the entropic term becoming unfavorable, reflecting a decreased degree of freedom. This entropic penalty is consistent with the view that D2 could induce preorientation effects that restrain the degree of liberty of the molecules, supporting the proposed mechanism by which D2 contributes to the interaction.

IFNγ D1 and D2 Domains Inversely Contribute to the Antiviral Activity of the Cytokine and to IFNγR Binding. Having established that D1 constitutes the actual HS binding

dx.doi.org/10.1021/ja4000867 | J. Am. Chem. Soc. 2013, 135, 9384−9390

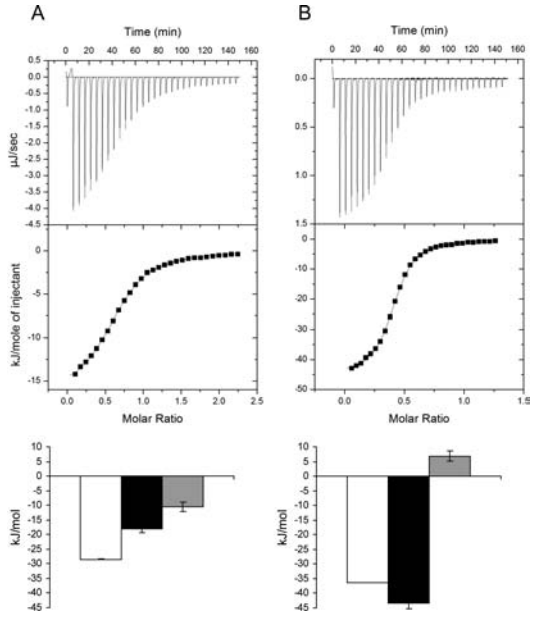

Figure 6. Binding isotherm for the interaction of IFNγ with heparin dp8. Heparin dp8 (112.5 and 1000 μM, respectively) was titrated into a solution of 100 μM of IFN$\gamma_{\Delta 136}$ (A) or 20 μM of IFNγ (B) in pH 7.2 phosphate buffer saline at 25 °C. For each panel, the upper part shows the peaks corresponding to the heat released from 30 automatic injections of 10 μL of dp8, and the middle panel shows the integrated peak area plotted as a function of the dp8/IFNγ molar ratio (squares). The solid line represents the best fit of the data, which was used to calculate the thermodynamic parameters, ΔG (white), ΔH (black), and $-T\Delta S$ (gray) shown on the lower part histograms (in kJ/mol).

site, whereas D2 functions essentially by maximizing the association rate of the interaction, we investigated how these two domains contribute to IFNγR binding and bioactivity. For this purpose, we used a SPR assay in which the IFNγR was immobilized on a streptavidin-coated sensorchip as previously described[24] and, in parallel, we measured the IFNγ concentration (IC_{50}) required to protect 50% of a cell monolayer from the vesicular stomatitis virus-induced cytolytic effect. We observed that IFNγ displayed an affinity of 0.13 ± 0.012 nM (Figures S6 and S7A in SI), a value identical to that reported from a radioligand binding assay with cell membrane-embedded IFNγR[34] and an IC_{50} of 35.3 ± 1.8 pM (Figure S7B in SI). Single-point mutations did not lead to important changes in affinity (from 0.8- to 2.4-fold compared to that for the wt cytokine) and increased bioactivity from 1.4- to 3.7-fold), resulting in enhanced K_D/IC_{50} ratio (Figure 7).

IFNγ_{SD2} and IFN$\gamma_{\Delta 136}$ displayed high affinity for the receptor as well (with K_D = 0.39 and 0.31 nM, respectively) and were more active than the wt-IFNγ, with IC_{50} of 8.1 pM for both mutants, giving rise to a 10−12-fold increase of the K_D/IC_{50} ratio compared to that of the wt cytokine. In contrast, IFNγ_{SD1}, in which all of the basic residues of the D1 domains were mutated, had a 10-fold decrease in affinity for IFNγR and was inactive (Figure S7 in SI and 7). Our analyses thus showed that, within the IFNγ carboxy-terminal sequence, D1 contributes both to bioactivity and IFNγR and HS binding, whereas D2, removal of which increases activity, is exclusively implicated in HS recognition.

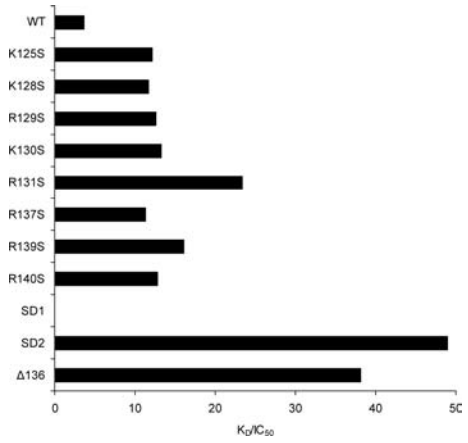

Figure 7. IFNγ binding to IFNγR and antiviral activity. The histogram shows the ratio between the IFNγ−IFNγR affinity (K_D determined from the data of Figure S6 in SI) and the antiviral activity for wt- and mutant-IFNγ shown in Figure S7 in SI).

CONCLUSION

The formation and dissociation of complexes involving proteins and HS are central to many biological processes, but the mechanism by which this occurs is poorly understood and is generally believed to rely on relatively low-specific electrostatic interactions. The present study shows that clusters enriched in basic amino acids, which commonly define HS binding sites, can contribute very differently to the binding process. Using IFNγ as a model system, our data showed that the binding to heparin of one of the two basic clusters (D1) that characterize the cytokine's carboxy-terminal sequence, is governed by favorable entropic and enthalpic contributions. The second cluster (D2), the presence of which induces the protein to bind heparin 10^2 faster, appeared to kinetically drive the interaction. These data suggest that heparin binding to IFNγ is a two-step process, in which close association is preceded by non-specific interactions that guide "diffusion to capture" of the protein. Such electrostatic steering mechanisms have been invoked to explain the fast association rate of a number of protein−protein or protein−DNA interactions but had yet not been experimentally reported for HS−protein complex formation.

The fact that the D2 domain mostly operates during the association phase but not in the formed complex has important functional consequences and helps to explain the mechanism by which heparin controls the activity of the cytokine. *In vivo*, unbound IFNγ is rapidly inactivated by extensive carboxy-terminal proteolysis that cleaves both the D1 and D2 domains.[20,35] However, HS bound to IFNγ limits the extent of the proteolytic degradations to the D2 domain only, thus enhancing the cytokine activity.[20,36,37] The D2 domain, in maximizing the association rate of IFNγ with HS, can thus be viewed as a motif enabling the cytokine to escape inactivation through D1 processing. The observation that HS triggers a rapid and almost quantitative accumulation within tissues of IFNγ which exists essentially in a bound form in nearby cells,[17,38] provides further credence to this proposed mode of action.

The question of how specific are the interactions between proteins and HS remains very open. The process we described here is likely to occur for many other HS-binding proteins. Interestingly, in particular, both of the cytokines that promote IFNγ synthesis (interleukins 12 and 18) and those that have the

dx.doi.org/10.1021/ja4000867 | J. Am. Chem. Soc. 2013, 135, 9384−9390

opposite effect (interleukins 4 and 10) are also GAG-binding proteins,[39−43] suggesting that these polysaccharides are closely associated to the regulation of this cytokine system.

Discriminating a first step, dictated by diffusion and long-range (nonspecific) interaction, from the final complex, should give rise to a better understanding of the mechanism by which amino acid basic clusters contribute to such interactions. As heparin-derived oligosaccharides are currently considered attractive pharmacological compounds,[44] this should help in the design of heparin-like structures that target protein−HS interfaces.

■ ASSOCIATED CONTENT

Supporting Information

Details concerning the sample preparation (IFNγ and oligosaccharides purification), the surface plasmon resonance procedures, the NMR assignment of the IFNγ amino acids resonances, the titration data, and the binding data analysis. This material is available free of charge via the Internet at http://pubs.acs.org.

■ AUTHOR INFORMATION

Corresponding Author

Hugues.Lortat-Jacob@ibs.fr

Present Address

[§]Stephane Sarrazin, Institut de Biologie et Chimie des Protéines, 7 passage du Vercors, 69007 Lyon, France.

Notes

The authors declare no competing financial interest.

■ ACKNOWLEDGMENTS

This work was supported by grants from Agence Nationale de la Recherche- ANR (ANR-09-PIRI-0009) and the Mizutani Foundation for Glycoscience. We thank the Partnership for Structural Biology-platforms for Biacore and NMR time and the Supercomping Center CECIC (http://cecic.cermav.cnrs.fr/) for the calculation.

■ REFERENCES

(1) Sarrazin, S.; Lamanna, W. C.; Esko, J. D. *Cold Spring Harbor Perspect. Biol.* **2011**, *3*, 1.
(2) Lindahl, U.; Li, J. P. *Int. Rev. Cell. Mol. Biol.* **2009**, *276*, 105.
(3) Mohammadi, M.; Olsen, S. K.; Goetz, R. *Curr. Opin. Struct. Biol.* **2005**, *15*, 506.
(4) Celie, J. W.; Beelen, R. H.; van den Born, J. *Front. Biosci.* **2009**, *14*, 4932.
(5) Handel, T. M.; Johnson, Z.; Crown, S. E.; Lau, E. K.; Proudfoot, A. E. *Annu. Rev. Biochem.* **2005**, *74*, 385.
(6) Lortat-Jacob, H. *Curr. Opin. Struct. Biol.* **2009**, *19*, 543.
(7) Sadir, R.; Imberty, A.; Baleux, F.; Lortat-Jacob, H. *J. Biol. Chem.* **2004**, *279*, 43854.
(8) Baker, N. A.; McCammon, J. A. *Methods Biochem. Anal.* **2003**, *44*, 427.
(9) Cardin, A. D.; Weintraub, H. J. *Arteriosclerosis* **1989**, *9*, 21.
(10) Lortat-Jacob, H.; Burhan, I.; Scarpellini, A.; Thomas, A.; Imberty, A.; Vives, R. R.; Johnson, T.; Gutierrez, A.; Verderio, E. A. *J. Biol. Chem.* **2012**, *287*, 18005.
(11) Lortat-Jacob, H.; Grosdidier, A.; Imberty, A. *Proc. Natl. Acad. Sci. U.S.A.* **2002**, *99*, 1229.
(12) Brooks, B.; Briggs, D. M.; Eastmond, N. C.; Fernig, D. G.; Coleman, J. W. *J. Immunol.* **2000**, *164*, 573.
(13) Camejo, E. H.; Rosengren, B.; Camejo, G.; Sartipy, P.; Fager, G.; Bondjers, G. *Arterioscler. Thromb. Vasc. Biol.* **1995**, *15*, 1456.
(14) Lortat-Jacob, H.; Kleinman, H. K.; Grimaud, J. A. *J. Clin. Invest.* **1991**, *87*, 878.
(15) Billiau, A.; Matthys, P. *Cytokine Growth Factor Rev.* **2009**, *20*, 97.
(16) Schoenborn, J. R.; Wilson, C. B. *Adv. Immunol.* **2007**, *96*, 41.
(17) Lortat-Jacob, H.; Brisson, C.; Guerret, S.; Morel, G. *Cytokine* **1996**, *8*, 557.
(18) Douglas, M. S.; Rix, D. A.; Dark, J. H.; Talbot, D.; Kirby, J. A. *Clin. Exp. Immunol.* **1997**, *107*, 578.
(19) Fluhr, H.; Spratte, J.; Heidrich, S.; Ehrhardt, J.; Steinmuller, F.; Zygmunt, M. *Fertil. Steril.* **2011**, *95*, 1272.
(20) Lortat-Jacob, H.; Baltzer, F.; Grimaud, J. A. *J. Biol. Chem.* **1996**, *271*, 16139.
(21) Lortat-Jacob, H.; Grimaud, J. A. *FEBS Lett.* **1991**, *280*, 152.
(22) Lescop, E.; Schanda, P.; Rasia, R.; Brutscher, B. *J. Am. Chem. Soc.* **2007**, *129*, 2756.
(23) Grzesiek, S.; Dobeli, H.; Gentz, R.; Garotta, G.; Labhardt, A. M.; Bax, A. *Biochemistry* **1992**, *31*, 8180.
(24) Sarrazin, S.; Bonnaffe, D.; Lubineau, A.; Lortat-Jacob, H. *J. Biol. Chem.* **2005**, *280*, 37558.
(25) Dolinsky, T. J.; Nielsen, J. E.; McCammon, J. A.; Baker, N. A. *Nucleic Acids Res.* **2004**, *32*, W665.
(26) Baker, N. A.; Sept, D.; Joseph, S.; Holst, M. J.; McCammon, J. A. *Proc. Natl. Acad. Sci. U.S.A.* **2001**, *98*, 10037.
(27) Felder, C. E.; Prilusky, J.; Silman, I.; Sussman, J. L. *Nucleic Acids Res.* **2007**, *35*, W512.
(28) Kalodimos, C. G.; Biris, N.; Bonvin, A. M.; Levandoski, M. M.; Guennuegues, M.; Boelens, R.; Kaptein, R. *Science* **2004**, *305*, 386.
(29) von Hippel, P. H.; Berg, O. G. *J. Biol. Chem.* **1989**, *264*, 675.
(30) Gabdoulline, R. R.; Wade, R. C. *Curr. Opin. Struct. Biol.* **2002**, *12*, 204.
(31) Myles, T.; Le Bonniec, B. F.; Betz, A.; Stone, S. R. *Biochemistry* **2001**, *40*, 4972.
(32) Perez Sanchez, H.; Tatarenko, K.; Nigen, M.; Pavlov, G.; Imberty, A.; Lortat-Jacob, H.; Garcia de la Torre, J.; Ebel, C. *Biochemistry* **2006**, *45*, 13227.
(33) Seyrek, E.; Dubin, P. *Adv. Colloid Interface Sci.* **2010**, *158*, 119.
(34) van Loon, A. P.; Ozmen, L.; Fountoulakis, M.; Kania, M.; Haiker, M.; Garotta, G. *J. Leukocyte Biol.* **1991**, *49*, 462.
(35) James, D. C.; Goldman, M. H.; Hoare, M.; Jenkins, N.; Oliver, R. W.; Green, B. N.; Freedman, R. B. *Protein Sci.* **1996**, *5*, 331.
(36) Döbeli, H.; Gentz, R.; Jucker, W.; Garotta, G.; Hartmann, D. W.; Hochuli, E. *J. Biotechnol.* **1988**, *7*, 199.
(37) Farrar, M. A.; Schreiber, R. D. *Annu. Rev. Immunol.* **1993**, *11*, 571.
(38) Fernandez-Botran, R.; Yan, J.; Justus, D. E. *Cytokine* **1999**, *11*, 313.
(39) den Dekker, E.; Grefte, S.; Huijs, T.; ten Dam, G. B.; Versteeg, E. M.; van den Berk, L. C.; Bladergroen, B. A.; van Kuppevelt, T. H.; Figdor, C. G.; Torensma, R. *J. Immunol.* **2008**, *180*, 3680.
(40) Hasan, M.; Najjam, S.; Gordon, M. Y.; Gibbs, R. V.; Rider, C. C. *J. Immunol.* **1999**, *162*, 1064.
(41) Lortat-Jacob, H.; Garrone, P.; Banchereau, J.; Grimaud, J. A. *Cytokine* **1997**, *9*, 101.
(42) Reeves, E. P.; Williamson, M.; Byrne, B.; Bergin, D. A.; Smith, S. G.; Greally, P.; O'Kennedy, R.; O'Neill, S. J.; McElvaney, N. G. *J. Immunol.* **2010**, *184*, 1642.
(43) Salek-Ardakani, S.; Arrand, J. R.; Shaw, D.; Mackett, M. *Blood* **2000**, *96*, 1879.
(44) Gandhi, N. S.; Mancera, R. L. *Drug Discovery Today* **2010**, *15*, 1058.